Available online at www.sciencedirect.com

SCIENCE DIRECT®

Journal of Volcanology and Geothermal Research 139 (2005) 103–115

Journal of volcanology and geothermal research

www.elsevier.com/locate/jvolgeores

Modeling of pyroclastic flows of Colima Volcano, Mexico: implications for hazard assessment

R. Saucedo[a,*], J.L. Macías[b], M.F. Sheridan[c], M.I. Bursik[c], J.C. Komorowski[d]

[a]*Instituto de Geología /Fac. Ingeniería UASLP, Dr. M. Nava No 5, Zona Universitaria, 78240 San Luis Potosí, Mexico*
[b]*Instituto de Geofísica, UNAM, Coyoacán 04510, D.F., México*
[c]*Geology Department, SUNY at Buffalo, Buffalo, NY 14260, USA*
[d]*Institut de Physique du Globe de Paris, Paris, Cedex 05, France*

Accepted 29 June 2004

Abstract

The 18–24 January 1913 eruption of Colima Volcano consisted of three eruptive phases that produced a complex sequence of tephra fall, pyroclastic surges and pyroclastic flows, with a total volume of 1.1 km^3 (0.31 km^3 DRE). Among these events, the pyroclastic flows are most interesting because their generation mechanisms changed with time. They started with gravitanional dome collapse (block-and-ash flow deposits, Merapi-type), changed to dome collapse triggered by a Vulcanian explosion (block-and-ash flow deposits, Soufrière-type), then ended with the partial collapse of a Plinian column (ash-flow deposits rich in pumice or scoria,). The best exposures of these deposits occur in the southern gullies of the volcano where Heim Coefficients (H/L) were obtained for the various types of flows. Average H/L values of these deposits varied from 0.40 for the Merapi-type (similar to the block-and-ash flow deposits produced during the 1991 and 1994 eruptions), 0.26 for the Soufrière-type events, and 0.17–0.26 for the column collapse ash flows. Additionally, the information of 1991, 1994 and 1998–1999 pyroclastic flow events was used to delimit hazard zones. In order to reconstruct the paths, velocities, and extents of the 20th Century pyroclastic flows, a series of computer simulations were conducted using the program FLOW3D with appropriate Heim coefficients and apparent viscosities. The model results provide a basis for estimating the areas and levels of hazard that could be associated with the next probable worst-case scenario eruption of the volcano. Three areas were traced according to the degree of hazard and pyroclastic flow type recurrence through time. Zone 1 has the largest probability to be reached by short runout (<5 km) Merapi and Soufrière pyroclastic flows, that have occurred every 3 years during the last decade. Zone 2 might be affected by Soufrière-type pyroclastic flows (~9 km long) similar to those produced during phase II of the 1913 eruption. Zone 3 will only be affected by pyroclastic flows (~15 km long) formed by the collapse of a Plinian eruptive column, like that of the 1913 climactic eruption. Today, an eruption of the same magnitude as that of 1913 would affect about 15,000 inhabitants of small villages, ranches and towns located within 15 km south of the volcano. Such towns

* Corresponding author. Tel.: +52 444 817 1039; fax: +52 444 811 1741.
E-mail address: rgiron@uaslp.mx (R. Saucedo).

0377-0273/$ - see front matter © 2004 Published by Elsevier B.V.
doi:10.1016/j.jvolgeores.2004.06.019

include Yerbabuena, and Becerrera in the State of Colima, and Tonila, San Marcos, Cofradia, and Juan Barragán in the State of Jalisco.

Keywords: hazard zonation; pyroclastic flows; Volcán de Colima; Mexico

1. Introduction

Colima Volcano lies in the western part of the Trans-Mexican Volcanic Belt (TMVB), a calc-alkaline continental arc that runs across the central part of Mexico. The western TMVB is widely accepted to be the result of subduction of the Cocos and Rivera Plates beneath the North American plate (Fig. 1A). The western TMVB consists of three regional structures: the Colima Graben, the Zacoalco right-lateral fault zone, and the Chapala Graben (CZC) (Luhr et al., 1985). The Colima graben is the southern arm of the CZC triple junction system. It is bordered by N–S normal faults running from the junction with the Chapala and Zacoalco grabens to the north and by the Pacific Ocean coast to the south (Fig. 1B). It is

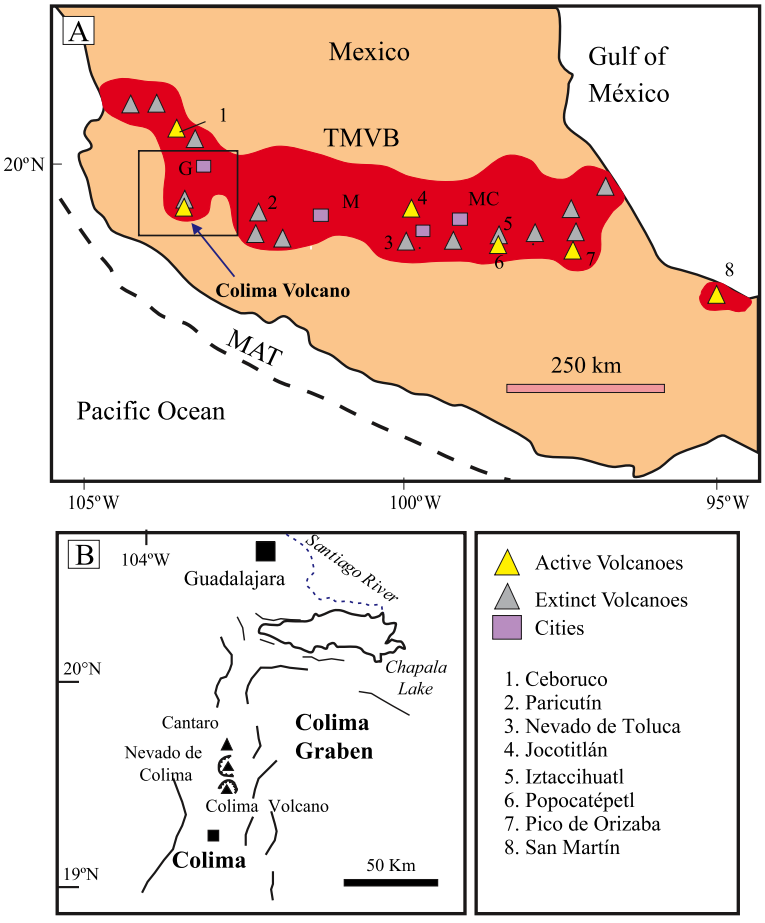

Fig. 1. (A) Location of Volcán de Colima in the western portion of the Trans-Mexican Volcanic Belt. Abbreviations are: MC=Mexico City, T=Toluca, G=Guadalajara, M=Morelia, TMVB=Trans-Mexican Volcanic Belt, and MAT=Middle American Trench. (B) Sketch map of the Colima Graben showing the location of the Cantaro, Nevado de Colima, and Colima volcanoes.

nearly 130 km long, and can be divided in two parts by the Mazamitla normal fault (Garduño and Tibaldi, 1991). The superposition of two tectonic regimes in this area, the subduction of the Rivera Plate and the rifting process taking place along the Colima Graben, has generated coeval alkaline and calc-alkaline volcanism during the last 4.6 Ma (Allan, 1986).

Colima Volcano (19°31′ N; 103°37′ W; 3850 m a.s.l.) is the southernmost active volcano of the Quaternary Cantaro–Nevado de Colima, and Colima Volcanic Complex. It is the most active volcano of Mexico in historic time with more than 43 eruptions since 1576 and is one of the most active volcanoes of North America, with at least 25 explosive eruptions in

Table 1
Summary of the historic reports and modern studies of volcanic activity at Colima Volcano, Mexico

Number	Year	Eruption type	References	Observations
1	1576	Possibly Plinian	Bárcena (1887)	Generation of block-and-ash flows (bafs)
2	1590	Explosion	Waitz (1935)	Important area covered by ash fall and likely generation of Soufrière-type bafs
3	1606	Possibly Plinian	Tello (1651); Arreola (1915)	The ash fall reach to Michoacan State and possible generation of Soufrière-type bafs
4	1611	Explosion	Bárcena (1887)	Important area was covered for ash fall and Soufrière-type bafs
5	1690	Possibly Plinian	Luhr and Carmichael (1990)	Possible generation of bafs
6	1771	Explosion	Bárcena (1887)	The ash fall reach the City of Guadalajara and possible generation of Soufrière-type bafs *
7	1818	Plinian	Sartorious (1869); Bárcena (1887); Arreola (1915)	Bafs and ash fall that reach Mexico City
8	1869–1972	Adventitious cone	Bárcena (1887)	Lava flow and Merapi-type bafs accompanied by ash fall
9	1880	Lava flow and Merapi-type bafs	Kerber, 1882 (personal communication C. Siebe)	Lava flows and Merapi-type bafs on the SW flank
10	1885–1986	Lava flow on the flank SW–W	Bárcena (1887)	Lava flow and Merapi type bafs
11	1885–1986	Explosion	Bárcena (1887)	Soufrière-type bafs?
12	1890	Explosion	Arreola (1915); De la Cruz-Reyna (1993)	The ash fall reached the City of Guanajuato and likely produced Soufrière-type bafs
13	1891–1992	Explosion	Arreola (1915); Starr (1903)	The ash fall reached the City of Colima and possible Soufrière-type bafs
14	1903	Explosion	Arreola (1915); Waitz (1935)	Ash fall and Soufrière-type bafs
15	1908	Explosion	Arreola (1915); Waitz (1935)	Ash fall and Soufrière-type bafs
16	1909	Explosion	Arreola (1915); Waitz (1935)	Ash fall and Soufrière-type bafs
17	1913	Plinian	Waitz (1915, 1935); Arreola (1915)	Merapi and Soufrière-types bafs derived from a Plinian column and ash fall that reached 725 km toward NE
18	1961–1962	Lava flow and Merapi-type bafs	Mooser (1961)	Merapi-type bafs on the southeast flank, runout 4.5 km
19	1975–1979	Lava flow and Merapi-type bafs	Thorpe et al. (1977)	Merapi-type bafs on the south flank, runout 1 km
20	1981–1982	Lava flow and Merapi-type bafs	Luhr and Carmichael (1991)	Merapi-type bafs on the north flank, runout 2 km
21	1987	Explosion	Luhr and Carmichael (1991)	Explosion crater and Soufrière-type bafs
22	1991	Lava flow and Merapi-type bafs	Rodríguez-Elizarrarás et al. (1991); Saucedo (2001)	Merapi-type bafs, 4 km runout and lava flow 2 km runout on southwestern flank
23	1994	Explosion	Saucedo et al. (1995)	Soufrière-type bafs, 3.5 km runout
24	1998–1999	Three lava flows and Merapi and Soufrière types bafs	Saucedo (2001)	Merapi-type bafs, 4.5 km runout, Soufrière-type bafs, 3.3 runout and lava flow 3 km runout
25	2001	Explosion and Soufrière-type bafs	Gavilanes, 2001 (personal communication)	Soufrière-type bafs, 2–3 km runout

the last 427 years (Luhr and Carmichael, 1981; Medina et al., 1983; De la Cruz-Reyna, 1993). Since 1576, Volcán de Colima has produced at least three Plinian eruptions similar to the 1913 type, 12 eruptions of Soufrière type, and at least 9 events of Merapi type (Saucedo et al., 2004) (Table 1).

Defining pyroclastic flow hazard at Volcán de Colima is an urgent problem due to its increased activity during the last decade. The path of such flows is not radial, but rather closely follows topography, since gravity drives them at high speeds down barrancas that have sources high on the volcano. The production of a large number of pyroclastic flows at Volcán Colima in November 1998 and July 1999 and during the huge explosions of May 10, February 10 and July 17, 1999, are significant in this regard. This activity appears to define a trend at this volcano where the quiet periods between events become shorter, and eruptions become increasingly more explosive with time. The danger of major pyroclastic flows and associated lahars increases at each stage of development of the edifice. There is a strong likelihood that a climactic series of eruptions like those of 1913 may occur shortly in the future. For this reason, it is important to understand the history of the climactic 1913 event and the distribution of its associated pyroclastic flows. This paper compares computer simulations of pyroclastic flows with the pattern of events during the 1913, 1991, 1994 and 1998–1999 events at this volcano.

2. Pyroclastic activity of the last decade

2.1. The 1991 eruption

Volcán de Colima is currently in a highly active state; the last decade was especially energetic with one eruption occurring every 3 years on the average. In 1991, following 10 years of calm, the volcano renewed its activity through a seismic crisis followed by magmatic activity (Núñez-Cornu et al., 1994; Lermo et al., 1993; Connor et al., 1991), which ended with the extrusion of an exogenous lava dome and the generation of small-volume block-and-ash flows (Rodríguez-Elizarrarás et al., 1991; Saucedo, 2001). These flows traveled down the Cordobán gullies (Central, East and West) for a distance of about 4 km from the summit. The line from the deposit terminus to the summit yielded a Heim Coefficient (H/L) of 0.44. The deposits of this episode had a maximum thickness of 8 m and a volume of 0.8×10^6 m^3 (Rodríguez-Elizarrarás et al., 1991); the total volume of 1.0×10^6 m^3 includes the fall deposits produced by the associated ash cloud (Saucedo et al., 2004).

2.2. The 1994 eruption

On July 4, 1994, a seismic swarm below the volcano signaled a renewal of activity (GVN, 1994, 1995). The activity increased in July 17 and culminated in July 21, with an explosion that destroyed the dome that formed during the 1991 eruption. This event excavated a 135-m diameter crater that was 40 m deep (GVN, 1994, 1995). The outburst generated block-and-ash flows that were channeled along the Central and West Cordobán gullies. These flows reached distances of 2 and 3.7 km from the summit, respectively. The deposits had a maximum thickness of 4 m and a minimum volume of 0.5×10^6 m^3 with a Heim Coefficient (H/L) of 0.44 (Table 2).

2.3. The 1998–1999 eruption

The most recent crisis started with a lava dome that began to form on November 20, 1998. By (November 21, 1998), the dome started to spill over the summit crater, forming slow moving lava flows that descended the volcano flanks (Navarro et al., 2002). Numerous pyroclastic flows formed by collapsing blocks from the lava flow fronts (Saucedo et al., 2002). These pyroclastic flows were able to enter the ravine heads and advance as far as 4.5 km from the summit H/L=0.40. This type of activity continued through January 1999. On February 10, 1999, a large explosion occurred destroying the summit dome and creating a new crater. The largest recorded explosion since 1913 occurred on July 17, 1999. This event produced a shock wave that was felt as far as 30 km from the volcano and formed a 10-km high volcanic plume above the summit. The production of significant pyroclastic flows in November 1998, February 1999, and July 1999 developed a pattern of short quiet periods followed by progressively more explosive events with time. This trend could support the

Table 2
Summary of pyroclastic flow activity occurred during the last century at Colima Volcano, Mexico

Year/Phase	Eruption type	Height in km	Runout in km	Heim H/L (a)	Volume (km^3)	Area (km^2)
1991	Merapi	1.8	4.0	0.44	0.0008	0.01
1994	Soufrière	2.5	3.8	0.44	0.00045	0.1
1998 Cordoban W	Merapi	1.9	4.5	0.40	0.0008	0.14
1998 Cordoban E	Merapi	1.4	3.0	0.47	0.00045	0.09
1999 Montegrande–San Antonio	Soufrière	1.5	3.3	0.45	0.00079	0.23
1999 La Lumbre	Soufrière	1.4	3.0	0.48	0.00036	0.09
1913 Phase I	Merapi	1.6	3.5	0.41	0.00013	0.07
1913 Phase II	Soufrière	1.4	9.5	0.26	0.01	0.23
1913 Phase III	Plinian	2.6	15.0	0.17	0.0019	0.45

Maximum assumed height for the volcano summit is 3,860 m a.s.l.

hypothesis that a climactic eruption like the 1913 might take place in the near future.

The deposits had an average thickness of 6 m and filled the Cordobán and the Montegrande–San Antonio gullies. Saucedo et al. (2002) estimated a total volume of 2.4×10^6 m^3. Most pyroclastic flows traveled about 3.5 km from the summit for which a H/L ratio of 0.45–0.48 was estimated.

3. Stratigraphic summary of the 1913 eruption

The following summary of the 1913 deposits is based on the work of Saucedo (1997), who constructed 192 stratigraphic sections. The deposit components mainly consist of juvenile (black scoria, pumice, and dense andesite), accidental lithics (light-gray altered andesite, tan pumice, and red altered andesite), free crystals, and glass. The stratigraphy from bottom to top contains the following units (Fig. 2):

F_1 (ca. 20 cm thick) is a light-gray matrix-supported block-and-ash flow deposit that mainly consists of dispersed angular accessory clasts with diameters up to 5 cm. It only crops out at El Cordobán East gully.

S_1 (1–3 cm thick) is a tan thinly stratified to massive surge deposit composed of fine ash. It mainly contains accessory red andesite lithics (light-gray, 95%; red altered andesite, 4.5%), and dense juvenile andesite (0.5%). It only extends to 2 km distance in the Cordobán East gully.

F_2 (7 cm thick) is a block-and-ash flow deposit composed of at least six flow units. It consists of accessory clasts set in an ash matrix. The component analysis of F_2 shows that 19% of this unit is made of dense juvenile andesite and 80% of accidental lithics represented by 74% of light-gray altered andesite and 6% of red altered andesites. This unit is exposed up to 3.2 km from the source.

F_3 (1.5–2.8 m thick) is a reddish block-and-ash flow deposit exposed in the West and East El Cordobán gullies and at El Playon in the northern part of the volcano. This unit overlies an erosion surface cut into F_2 and is a useful stratigraphic marker for the 1913 eruption. It is composed of accessory clasts set in an ash matrix with a notable abundance of red altered andesitic clasts that makes up only 34% of the deposit.

C_1 (average thickness 15 cm) is a gray clast-supported fallout layer composed of lapilli to coarse ash accessory clasts and minor pumice. It has an approximate dispersal axis oriented 36° NE, with an average thickness of 4–8 cm at a distance of about 10 km from the summit.

S_2 (up to 30 cm thick) is a pale-gray to pinkish laminated surge layer rich in accessory clasts that overlies an erosion surface in layer C_1. This layer is exposed in all gullies around the volcano.

F_4 (up to 7 cm thick) is a pale-gray block-and-ash flow deposit composed of lapilli-sized lithics supported in an ash matrix. It consists of a series 2 or 3 flow units that show a gradual decrease in clasts-sizes away from the volcano. F_4 is widely exposed at all gullies around the volcano up to 12 km from the summit.

C_2 is a clast-supported tan pumice-rich fallout layer and represents the most important bed of the 1913

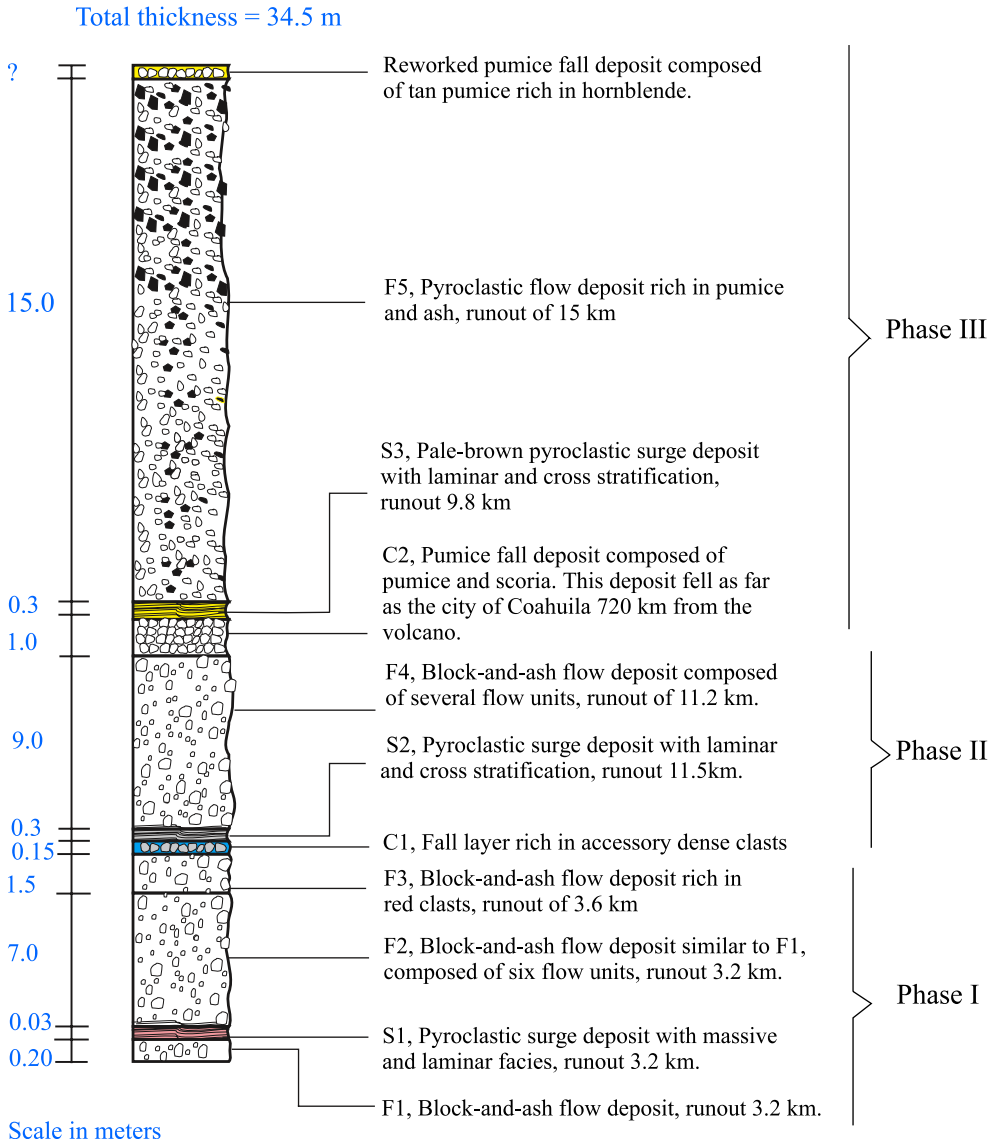

Fig. 2. Composite stratigraphic section of the 1913 deposits according to Saucedo (1997).

deposits. It has a dispersal axis of 30°NE with a thickness of 1 m (ca. 2 km from the source), 15 to 32 cm at ca. 32 km, ~0.5 cm at 125 km, and it was <1 mm thick at the City of Saltillo, 725 km from the source, as reported by Waitz, 1915.

S_3 (variable thickness of 0.3–40 cm) is a light-brown, laminated surge deposit with cross-bedded structures. It has discrete discontinuous cross-stratified horizons with accretionary lapilli at a distance of 2.4 km SW from the volcano summit.

F_5 is a brown ash-flow deposit, rich in pumice, with dispersed lapilli-size pumice and scoria clasts. It contains at least three flow units with a general upward increase in scoria (65% to 82%) while pumice decreases from 33% to only 1%. F_5 is widely distributed around the volcano to a distance of 15 km from the source, notable in the outskirts of the towns of Queseria, Tonila and San Marcos. These distal exposures correlate to the eruption descriptions of Waitz (1915, 1935).

4. Chronology of the 1913 eruption

Prior to 1913, Colima Volcano had an altitude between 3860 and 3960 m (Waitz, 1915; Arreola, 1915) and a dome of lava blocks occupied its summit. These features formed during activity occurring between 1903 and 1909 (Waitz, 1915) (Fig. 3). Colima Volcano began its climactic phase of explosive eruptions in January 1913 (Waitz, 1915). According to Saucedo (1997), this event can be separated into three main eruptive phases, each one producing a characteristic sequence of deposits as shown in the composite stratigraphic section (Fig. 2). The chronology of the 1913 eruption can be summarized as follows.

The first phase of the eruption started on January 18 or 19 with Merapi type activity that produced the gravitational collapse of the external parts of the dome with the generation of (Merapi-type) block-and-ash flows and surges, which traveled as far as 4 km from the summit (Fig. 4A). The deposits left by these explosions are exposed in the El Cordobán gullies (F_1, S_2, F_2 and F_3 in Fig. 2).

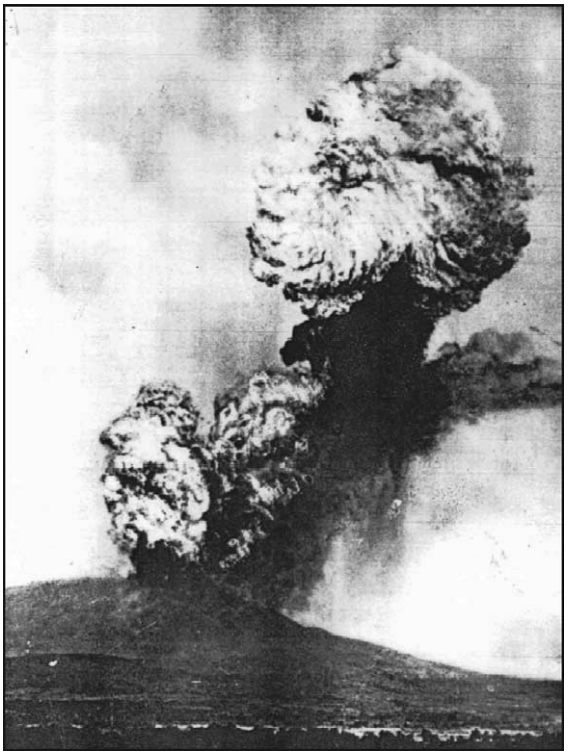

Fig. 3. Photograph of the activity recorded in 1909 at Volcán de Colima that shows the generation of pyroclastic flows (Courtesy of Mr. Velasco Murgía, 1995).

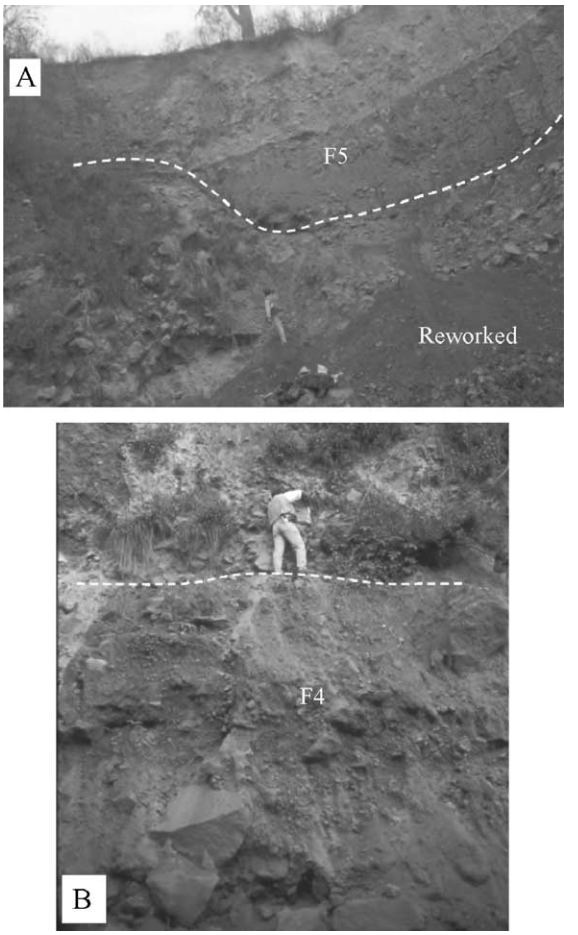

Fig. 4. Photograph of two types of pyroclastic flow deposits: (A) pyroclastic flow deposit rich in pumice and ash, and (B) Soufrière-type block-and-ash flows.

The second phase of the 1913 eruption began on January 20 (between 4:30 and 11:30 AM; local time) with a Vulcanian-type explosion that destroyed large parts of the summit dome. This event produced a lithic-rich fallout (C_1) dispersed mainly to the NE, a basal surge deposit (S_2), and the collapse of the column forming Soufriere-type block-and-ash flows (Hay, 1959), that filled the gullies in the southern slopes of the volcano up to a distance of 10 km (F_4, Fig. 4B).

The activity peaked on January 20 (phase III) with the production of a plinian eruption column that rose ca. 21 km above the crater and was dispersed by the predominant winds to the NE. This column was

Fig. 5. Jagged morphology of the Colima crater after the 1913 eruption, the crater is about 400 m in diameter. Photograph by Ortiz (1944).

sustained during a period of 8 h, producing widespread andesite pumice fallout with a maximum thickness of 1 m (C2). The deposit covered an area of ca. 14,100 km^2 and was over 1 km^3 (0.31 km^3 DRE) in volume (Saucedo, 1997). Ash fell as far as 725 km to the NE for several days (Waitz, 1915). Partial collapses of the plinian column generated a basal surge (S_3) and ash flows rich in pumice (F_5). These were witnessed to travel up to 15 km from the summit (F_5). The pyroclastic flow deposits are rich in hornblende–andesite banded scoria (Luhr and Carmichael, 1990; Robin et al., 1991). The intensity of the eruption declined during the night of January 20 and ended on January 24. A total volume of the 0.31 km^3 DRE was produced during the 1913 eruption in contrast with 0.001 km^3 for the 1991 dome collapse flow deposits (Rodríguez-Elizarrarás et al., 1991).

The 1913 eruption removed about 100 m of the existing edifice and left a summit crater that was 450 m in diameter and at least 350 m deep (Waitz, 1935). This crater had a very irregular jagged outline (Fig. 5).

5. Modelling of pyroclastic flows

To model the Volcán de Colima pyroclastic flows, we used the 1913 eruptive phases described above as an initial reference set (Table 2), as follows.

Phase I, Merapi-type block-and-ash flows (H/L=0.41) similar to flow deposits produced during the 1991, 1994, and 1998–1999 eruptions. These flows result from the gravitational collapse of external parts of the summit dome or by the collapse of advancing lava flow fronts. These types of flows generally do not travel farther than 4 km from the summit and most just barely reach the break in the slope at the volcano apron.

Phase II, produces Soufriere-type block-and-ash flows (H/L=0.26). These flows have a radial path and may travel up to 9.5 km from the source. The July 17, 1999, explosion produced a 3.3-km-long pyroclastic flow that filled both the Montegrande and San Antonio ravines.

Phase III, generated column collapse ash flows rich in pumice and scoria (H/L=0.17–0.26) similar to the flows described during the fountain collapse of phase III of the 1982 eruption of El Chichón Volcano (Macías et al., 1997). These flows are the product of the partial or total collapse of a plinian column and therefore they have a higher initial kinetic energy that is a function of their greater initiation height. At Colima, these flows are able to reach up to 15 km from the summit and show a general decrease in their clast diameter in direction of the flow.

5.1. Flow-3D modeling of pyroclastic flows

Flow models are useful to forecast the surficial movement of pyroclastic materials driven by gravity. The kinetic model (FLOW3D) used here was developed by Kover (1995). It uses a detail topographic data base of the volcano for which it closely mimics the trajectories of flows and therefore represents a useful tool in volcanic risk assessment. This model is based on the algorithm of Mellor (1978) for snow avalanches. It uses three empirical parameters to mimic the basal friction (a_0), internal resistance to flow (a_1), and external resistance (a_2) due to turbulence.

In order to reconstruct the paths, velocities, and extents of the 1913, 1991, 1998–1999 pyroclastic flows, an iterative series of computer simulations were conducted with the program FLOW3D (Kover, 1995) using appropriate frictional coefficients (a_0) and apparent viscosities (a_1). In all cases, the external resistance (a_2) was assumed to be zero and the viscous parameter (a_1) to have a value of 0.01 because higher figures rapidly decelerated simulated flows constraining them to stop. In the case of the basal friction (a_0) parameter, we used different values that attempt to reproduce the basal

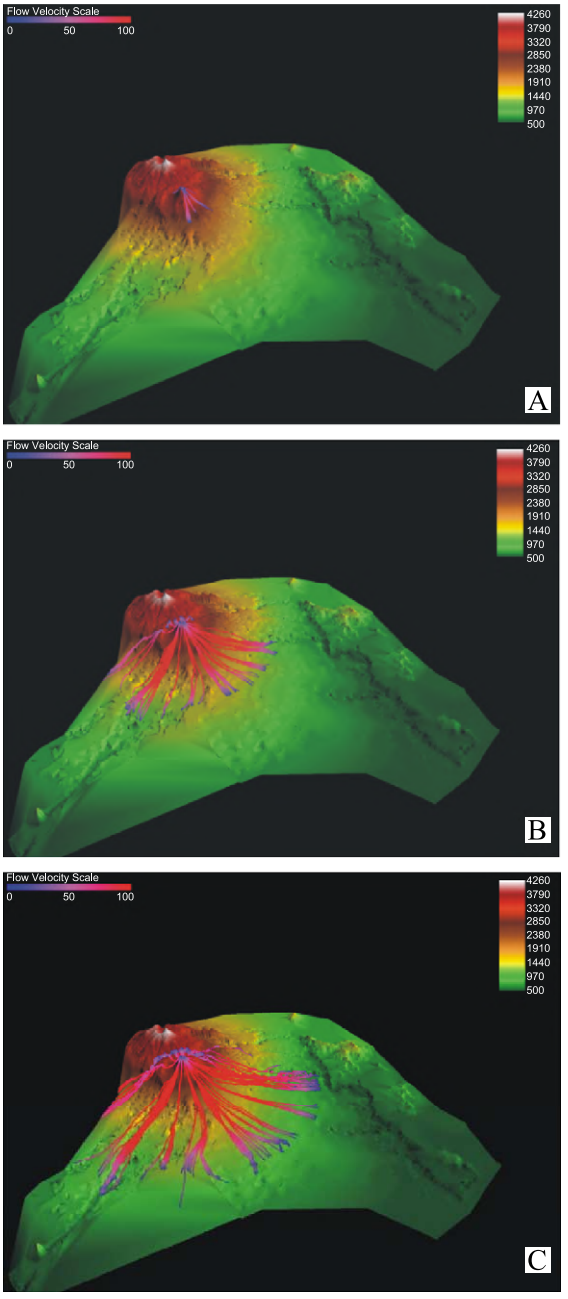

Fig. 6. Modeling of different types of pyroclastic flows compared to their maximum runout in the field. (A) Merapi-type pyroclastic flows, (B) Soufriere-type pyroclastic flows, and (C) Column collapse pyroclastic flows. The vertical numbered bars in the upper-right corner of the images represent vertical elevations in the Digital Elevation Model.

friction exerted by preexisting topographic and other ground irregularities that reduce the velocity of the moving flows.

For flows of Merapi-type and phase I of the 1913 eruption, a good fit with field parameters was obtained with a frictional parameter (a_0) of 0.35 (Fig. 6A). The simulated flows had a runout of 3.5 km with a maximum velocity between 30 and 68 m/s. The total runout time was 160 s.

The Soufrière Type and phase II simulated flows best mimic the deposits with a frictional parameter (a_0) of 0.17 (Fig. 6B). The simulated flows had a runout of 8.2 km with a maximum velocity of 55 to 100 m/s. The runout time for these flows was 160 s.

For partial collapse of Plinian column or phase III, simulations fitted the actual deposits with a frictional parameter (a_0) of 0.12 (Fig. 6C). These simulations had a maximum runout of 13 km with a maximum flow velocity of 60 to 110 m/s. The calculated runout time for these flows was 224 s.

6. Hazard zonation of pyroclastic flows

By incorporating the modeled flow paths of the three types of pyroclastic flows, a three-zone hazard map has been constructed, to complement the existing hazards maps of Volcán de Colima (Del Pozzo et al., 1995; Sheridan and Macías, 1995). Its construction was also supplemented by an analysis of its historic record for the last 427 years.

The simulation of the different pyroclastic flows shows a good correlation with the data collected in the field. The model predicts that all ravines descending from the volcano are susceptible to be filled by different types of pyroclastic flows. Nevertheless, depending on the type of pyroclastic flows generated, there would be three different areas affected as follows (Fig. 7). These areas would have a completely different aspect if we just have traced simple circles around the volcano based on H/L ratios obtained from lengths of past flows.

6.1. Red zone

For Merapi-type pyroclastic flows, the model predicts that they might advance up to ~7 km from the summit following the main ravines located in the

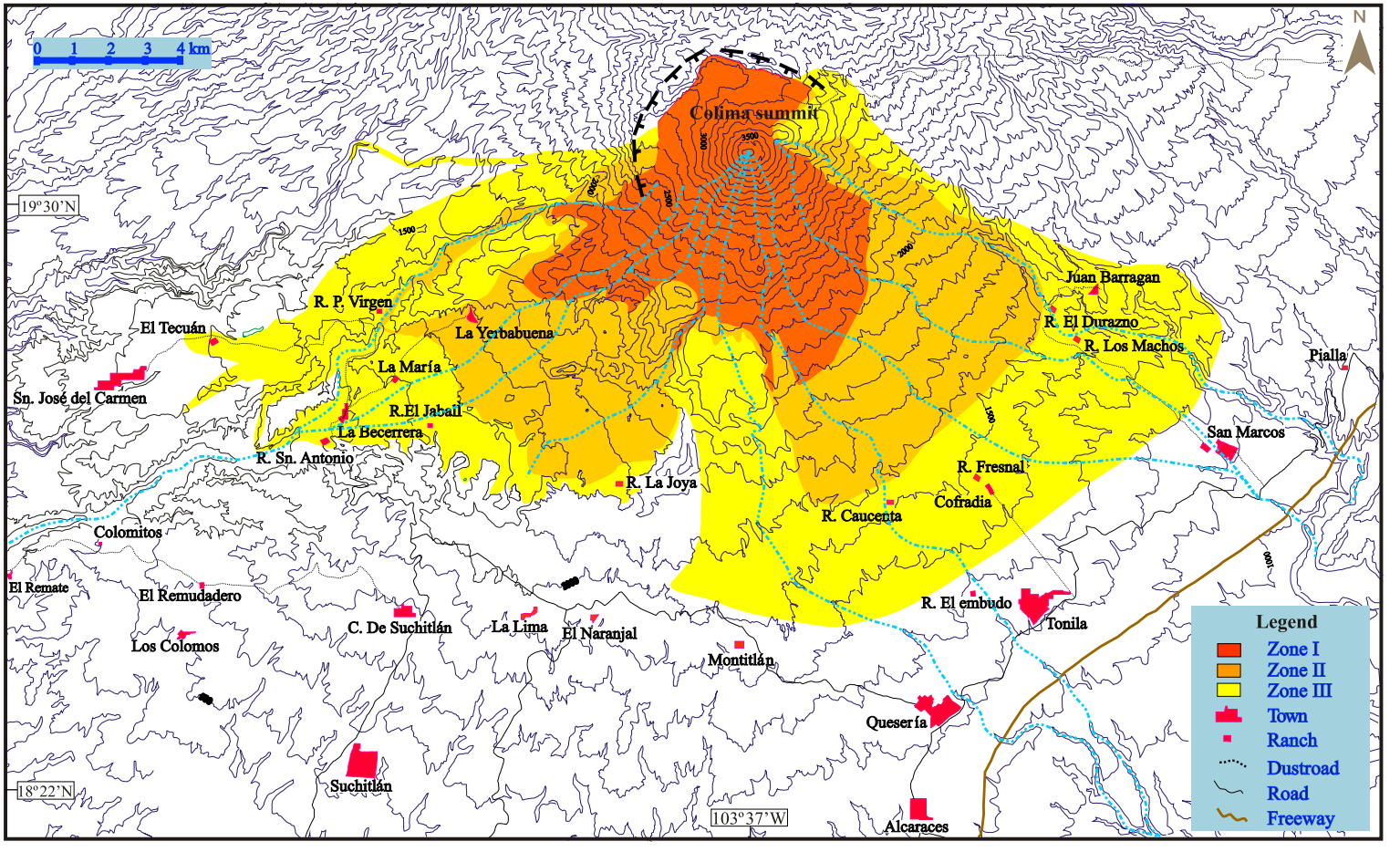

Fig. 7. Hazard map for pyroclastic flow deposits of Colima Volcano showing distinct eruptive scenarios depicted in three zones: red zone for Merapi-type pyroclastic flows, orange zone for Soufriere-type pyroclastic flows, and yellow zone for column collapse pyroclastic flows.

SW sector of the volcano (La Lumbre and Zarco). In the gullies located in the S–SE sector of the volcano (Montegrande, El Muerto, La Tuna and Santa Ana), the flows might reach up to 6 km from the summit, and in all remaining gullies, the flows would travel distances of 5 km. During the last decade, this type of pyroclastic flows has occurred every 3 years and no people has been affected by such phenomena.

6.2. Orange zone

The Soufrière-type pyroclastic flows could reach a distance of 11 km in gullies located on the SW flank of the volcano (La Lumbre, Zarco and Cordobán), 9–10 km in gullies located on the S–SE flanks (Montegrande, El Muerto, La Tuna, Santa Ana, Arena and Beltrán), whereas to the north, they could completely cover the Playón area, located between Volcán de Colima and the Paleofuego Caldera. This flow type has occurred many times during the volcanic history of Colima, but pyroclastic flows with a ~10-km runout have only occurred every ~100 years.

6.3. Yellow zone

Pyroclastic flows derived by the collapse of Plinian columns (1913-type) could reach distances of 12–17 km on the SW part of the volcano, 12–14 km on the SE part, and 11 km in the W part (Fig. 7). The model showed that these flows might able to surmount the western and eastern portions of the Paleofuego Caldera, affecting the Tecuán, San José del Carmen, and Juan Barragán villages. These data are considered to be of great importance, because these towns are located outside the hazard zones of pyroclastic flows in the hazards map of Del Pozzo et al. (1995). Because of the difficult access to these areas and the problematic distinction between deposits generated by the modern Volcán de Colima and those derived from the Paleofuego Volcano, this model becomes a useful tool to better delimit areas with a potential hazard for pyroclastic flows (Fig. 7). This type of flow has taken place only twice during the last 185 years. During the 1913 eruption, eight people were killed, but today due to population growth around the volcano in the last century, this type of pyroclastic flow would directly affect up to 15,000 people.

7. Limitations of the map

It is noteworthy to mention that the stratigraphic sequence of Volcán de Colima records important ash-flow deposits which are likely associated with larger volcanic events than the 1913 eruption. These brown ash-flow deposits are well exposed around the volcanic edifice but have not been ascribed yet to specific eruptions. Therefore our hazard zone based upon the 1913 column collapse event, does not consider such larger magnitude events (i.e., does not include the true "cataclysmic" events possible from this volcano).

The hazard zonation does not consider the associated pyroclastic surge clouds that accompanied the basal avalanche part of the dense pyroclastic flows (Rose et al., 1977; Davies et al., 1978; Nairn and y Self, 1978). The more dilute and turbulent surge clouds might be capable of surmounting topographic barriers as demonstrated by historic eruptions as the 1902 Mont Pelée eruption (Lacroix, 1904; Fisher and Heiken, 1982), the 1980 Mount St. Helens eruption (Mellors et al., 1988; Denlinger, 1987), and the 1991 Mt. Unzen eruption (Fujii and Nakada, 1999; Miyabuchi, 1999). A numerical model considering the maximum runouts of these clouds was proposed by Takahashi and Tsujimoto (2000). In light of this lack of information, we assume that the maximum runout of pyroclastic surge found beyond the limits of their parental pyroclastic flows is similar to that of the 1998–1999 events, i.e. approximately 500 m, although pyroclastic surges associated to major large collapse events might be capable to outreach the basal avalanche at distances larger than 1 km.

8. Discussion and conclusions

The stratigraphy of the 1913 eruption deposits suggests that this event occurred with three main eruptive stages, each one producing different types of gravity-driven pyroclastic flows. Data from this eruption, along with the deposit records from 1991, 1994, and 1998–1999 events, provide a solid basis for modeling the areas and levels of pyroclastic flow hazard that could be associated with the next probable maximum scenario eruption of the volcano. They also yield parameters that could be used by FLOW3D for real-time analysis during the next volcanic crisis at Colima.

8.1. Risk of a future larger event

In the historic pattern of activity at Colima, each eruption reaches a climactic phase in an approximate 100-year cycle. Pyroclastic flows associated with such an event present a grave danger to the villages at the foot of the volcano. The hazards map of Volcán de Colima (Del Pozzo et al., 1995) gives a general idea of the areas that could be affected by these flows, and other types of volcanic events. In addition, Sheridan and Macías (1995) produced a hazards map based on probabilities for the occurrence of small-volume pyroclastic flows such as those studied in this work.

The timing of major pyroclastic flow production at Volcán de Colima is extremely difficult to forecast, as exemplified by the April 1991 pyroclastic flows that occurred just 3 weeks after the level of risk was formally lowered because of a decrease in the seismicity. It is obvious that pyroclastic flow production may not be related to seismicity or other geophysical parameters that are currently monitored at the volcano. Rather gravitational instability is a major factor in their production and character. Stability can be best monitored by detailed and consistent field observations of features such as the development of cracks, growth in lava accumulation at the summit, or other factors.

Because of the uncertainty involved in forecasting the climactic events of eruption cycles at Colima, we must be sure not to underestimate the potential of a sudden destructive event. In fact, the terminal phase of this cycle could be at hand in the present eruptive phase, or could occur in the next few years. We are unable to determine future events at the volcano without uncertainty and present monitoring may not be able to give sufficient lead-time for civil action.

Presently several villages are at risk at different levels of probability to the hazard of pyroclastic flows and their associated ash clouds. The effect of the ash clouds commonly exceeds the limits predicted from the existing locations of deposits of similar events. Examples of under prediction of ash clouds and pyroclastic flows are at Mount St. Helens in 1980, El Chichón in 1982, Unzen in 1991, and Pinatubo in 1991. The maximum event (1913-type) expected at Volcán de Colima would have a high probability of affecting many villages. Besides Yerbabuena, which has a risk probability of about 99% under the Merapi and Soufriére type events (Sheridan and Macías, 1995), high risk is associated with La Becerrera, San Antonio, El Naranjal, Atenguillo, El Fresnal, and San Marcos. Ash clouds associated with pyroclastic flows could potentially affect Tonila and Queseria villages.

Acknowledgments

This research was supported by grants PROMEP (UASLP-PTC-56 to R. Saucedo), CONACYT (27993-T and 38586-T to J.L. Macías), NSF (EAR-0087665 and ACI-0121254 to M.F. Sheridan), and (EAR9725361 to M.I. Bursik). We are indebted to L. Capra for her support during computer modeling, and with A. Cortés, and J.C. Gavilanes for their support during field work. We thank the fruitful comments by two anonymous reviewers.

References

Allan, F.J., 1986. Geology of Northern Colima and Zacoalco grabens, Southwest Mexico: Late Cenozoic rifting in the Mexican volcanic belt. Geological Society of America Bulletin 97, 473–485.

Arreola, J.M., 1915. Catálogo de las erupciones antiguas del volcán de colima. Memorias de la Sociedad Cientifica "Antonio Alzate" 32, 443–481.

Bárcena, M., 1887. Informe sobre el estado actual del Volcán de Colima. Naturaleza (Periódico Científico de la Sociedad Mexicana de Historia Natural). 2ª serie, tomo 1.

Connor, C., Luhr, J., Del Pozzo, A., 1991. Structure and petrology of the march 1991 dome, volcán Colima, México: possible transition toward explosive eruption. Geophysical Research Letters, 1–13.

Davies, D.K., Quearry, M., Bonies, S.B, 1978. Glowing avalanches from the 1974 eruption of the volcano Fuego de Guatemala. Geological Society of America Bulletin 89, 369–394.

De la Cruz-Reyna, S., 1993. The historical eruptive activity of Colima Volcano, México. Journal of Volcanology and Geothermal Research 55, 51–68.

Del Pozzo, A.L., Sheridan, M.F., Barrera, D., Hubp, J.L, Selem, L.V, 1995. Potential hazards from Colima Volcano, México. Geofísica Internacional 34, 363–376.

Denlinger, R.P., 1987. A model for generation of ash clouds by pyroclastic flows, with application to the 1980 eruptions at Mount St. Helens. Journal of Geophysical Research 92, 10,284–10,298.

Fisher, R.V., Heiken, G., 1982. Mt. Pelée, Martinique: May 8 and 20, 1902, pyroclastic flows and surges. Journal of Volcanology and Geothermal Research 13, 339–371.

Fujii, T., Nakada, S., 1999. The 15 September 1991 pyroclastic flows at Unzen volcano (Japan): a flow model for associated ahs-cloud surge. Journal of Volcanology and Geothermal Research 89, 159–172.

Garduño, V., Tibaldi, A., 1991. Kinematic evolution of the continental active triple junction of the western Mexican Volcanic Belt. Comptes Rendus De l'Academie des Sciences 30, 1–6.

GVN, 1994. Bulletin of Global Volcanism Network, vol. 19 (8). Smithsonian Institution, Washington, DC, pp. 12–13.

GVN, 1995. Bulletin of Global Volcanism Network vol. 20 (2). Smithsonian Institution, Washington, DC, pp. 9–10.

Hay, R.L., 1959. Formation of the Crystal-Rich Glowing Avalanche Deposits of Soufriere. BWI.

Kerber, E., 1882. Eine Besteigung des tätigen Vulkanus vo Colima. In: Aus allen Welttheilen, 14, Nov. P.33–39.

Kover, T.P., 1995. Application of a digital terrain model for the modeling of volcano flows: a tool for volcanic hazard determination. MA thesis, SUNY at Buffalo, 62 pp.

Lacroix, A., 1904. La Montagne Pelée et ese éruptions. Massons et Cie, Paris, p. 622.

Lermo, J., Cuenca, J., Monfret, T., Hernández, F., Nava, E., 1993. Algunas características espectrales de la sismicidad asociada a la actividad del Volcán de Colima. Geofisica Internacional 32 (4), 683–697.

Luhr, J.F., Carmichael, I.S.E., 1981. Colima: history cyclicity of eruptions. Volcano News 7, 1–3.

Luhr, J.F., Carmichael, I.S.E., 1990. Geology of volcán de Colima. Boletin - Instituto de Geologia. Universidad Nacional Autonoma de Mexico 107, p. 101.

Luhr, J.F., Nelson, S.A., Carmichael, I.S.E., 1985. Active rifting in southwestern México-manifestations of on incipient eastward spreading ridge jump. Geology 13, 54–57.

Macías, J.L., Sheridan, M.F., Espíndola, J.M., 1997. Reappraisal of the 1982 eruptions of El Chichón volcano, Chiapas, Mexico New data from proximal deposits. Bulletin of Volcanology 58, 459–471.

Medina, F., De la Cruz, S., Mena, M., 1983. El Volcán de Colima. Instituto de Geofisica, UNAM, reporte 11–18.

Mellor, M., 1978. Dynamics of snow avalanches. In: Voight, B. (Ed.), Rockslides and Avalanches 1: Natural Phenomena. Elsevier, Amsterdam, pp. 753–792.

Mellors, R.A., Waitt, R.B., Swanson, D.A., 1988. Generation of pyroclastic flows and surges by hot rock avalanches from the dome of Mount St Helens volcano, USA. Bulletin of Volcanology 50, 14–25.

Miyabuchi, Y., 1999. Deposits associated with the 1990–1995 eruption of Unzen volcano. Journal of Volcanology and Geothermal Research 89, 139–158.

Mooser, F., 1961. Los volcanes de Colima. Bol. Inst. Geol. UNAM 61, 49–71.

Nairn, I.A., y Self, S., 1978. Explosive eruption and pyroclastic avalanches from Ngauruhoe in February 1975. Journal of Volcanology and Geothermal Research 3, 39–60.

Navarro, C., Gavilanes, J.C., y Cortés, A., 2002. Movement and emplacement of lava flow at Volcán de Colima, Mexico: Nov. 1998–Feb. 1999. Journal of Volcanology and Geothermal Research 117, 155–167.

Núñez-Cornu, F., Nava, A., De la Cruz, S., Jiménez, Z., Valencia, C., García, R., 1994. Seismic activity related to the 1991 eruption of Colima volcano, Mexico. Bulletin of Volcanology 56, 228–237.

Ortiz, S.G., 1944. La zona volcánica "Colima" del Estado de Jalisco. Insituto de Geografía, Universidad de Guadalajara, p. 44.

Robin, C., Camus, G., Gourgaud, A., 1991. Eruptive and magmatic cycle at Fuego de Colima Volcano (México). Journal of Volcanology and Geothermal Research 45, 209–225.

Rodríguez-Elizarrarás, S.R., Siebe, C., Komorowski, J.C., Espíndola, J.M., Saucedo, R., 1991. Field observations of pristine block and ash flow deposits emplaced on April 16–17, at Volcán de Colima, Mexico. Journal of Volcanology and Geothermal Research 48, 399–412.

Rose, W.I., Pearson, T., Bonis, S., 1977. Nuée ardente eruption the foot of a dacite lava flow Santiaguito, Guatemala. Bulletin of Volcanology 40 (1), 23–38.

Sartorious, C., 1869. Eruption of the Volcano of Colima in June 1869. Smithsonian Report, p. 423.

Saucedo, G.R., 1997. Reconstrucción de la erupción de 1913 del volcán de Colima. MS Thesis, México D.F., Instituto de Geofísica, UNAM, 185 pp.

Saucedo, R., 2001. Erupciones de 1991 y 1998–1999 del Volcán de Colima: Mecanismos de transporte y depositación de los flujos piroclásticos de bloques y ceniza. PhD thesis, UNAM, México, D.F.

Saucedo, R., et al., 1995. Internal Report Observatorio Vulcanológico de la Universidad de Colima, p. 35.

Saucedo, R., Macías, J.L., Bursik, M.I., Gavilanes, J.C., Cortés, A., 2002. Emplacement of pyroclastic flows during the 1998–1999 eruption of volcán de Colima, México. Journal of Volcanology and Geothermal Research 117, 129–153.

Saucedo, R., Macías, J.L., Bursik, M.I., 2004. Pyroclastic flow deposits of the 1991 eruption of Volcán de Colima, Mexico. Bulletin of Volcanology 66, 291–306.

Sheridan, M.F., Macías, J.L., 1995. Estimation of risk probability for gravity-driven pyroclastic flows at Volcán Colima, México. Journal of Volcanology and Geothermal Research 66, 251–256.

Starr, F., 1903. The recent eruptions of Colima. J. Geol. 11, 750.

Takahashi, T., y Tsujimoto, H., 2000. A mechanical model for Merapi-type pyroclastic flow. Journal of Volcanology and Geothermal Research 98, 91–115.

Tello, F.A., 1651. Libro segundo de la Crónica Miscelanea en que se trata de la conquista espiritual y temporal de la Santa Provincia de Jalisco en el Nuevo Reino de la Galicia y Nueva Vizcaína y Descubrimiento del nuevo México.., Imprenta de la República Literaria, Guadalajara.

Thorpe, R.S., Gibson, I., Vizcaino, J., 1977. Andesitic pyroclastic flows from Colima Volcano. Nature 265, 724–725.

Waitz, P., 1915. El estado Actual de los Volcanes de México y la Última Erupción del Volcán de Colima (1913) Revista Volcanológica, pp. 259–268.

Waitz, P., 1935. Datos históricos y bibliográficos acerca del Volcán de Colima. Memorias de la Sociedad Cientifica "Antonio Alzate" 53 (9–10), 349–383 (tomo).